communications earth & environment

ARTICLE

https://doi.org/10.1038/s43247-023-00779-5 OPEN

Quantitative characterization of orogens through isotopic mapping

Tao Wang[1,2]✉, Wenjiao Xiao[3]✉, William J. Collins[4], Ying Tong[1,2], Zengqian Hou[2], He Huang[2], Xiaoxia Wang[5], Shoufa Lin[6], Reimar Seltmann[7], Chaoyang Wang[2] & Baofu Han[8]

The relationship between orogens and crustal growth is a fundamental issue in the Earth sciences. Here we present Nd isotope mapping results of felsic and intermediate igneous rocks from eight representative and well-studied Phanerozoic orogens. The results illustrate the distribution of isotopic domains that reflect the compositional architecture of the orogens. We calculated the areal proportion of juvenile crust and divided the orogens into five types: (i) highly juvenile (with >70% juvenile crust); (ii) moderately juvenile (70–50%; e.g., the Altaids with ~58% and the North American Cordillera with ~54%); (iii) mixed juvenile and reworked (50–30%; e.g., the Newfoundland Appalachians with ~40% and the Lachlan Orogen with ~31%); (iv) reworked (30–10%); (v) highly reworked (<10%; e.g., the Tethyan Tibet (~3%), Caledonides (~1%), Variscides (~1%), and the Qinling-Dabie Orogen (<1%)). This study presents an approach for quantitatively characterizing orogens based on compositional architecture through isotope mapping, and for investigating the relationships between orogenesis and continental growth.

[1] Beijing SHRIMP Center, Institute of Geology, Chinese Academy of Geological Sciences, Beijing, China. [2] Key Laboratory of Earthprobe and Geodynamics, Chinese Academy of Geological Sciences, Beijing, China. [3] National Key Laboratory of Ecological Safety and Sustainable Development in Arid Lands, Xinjiang Institute of Ecology and Geography, Chinese Academy of Sciences, Urumqi, China. [4] School of Earth and Planetary Sciences, Curtin University, Perth, Australia. [5] Institute of Mineral Resources, Chinese Academy of Geological Sciences, Beijing, China. [6] Department of Earth and Environmental Science, University of Waterloo, Waterloo, Canada. [7] Centre for Russian and Central EurAsian Mineral Studies, Natural History Museum, London, UK. [8] Ministry of Education Key Laboratory of Orogenic Belts and Crustal Evolution, School of Earth and Space Sciences, Peking University, Beijing, China. ✉email: taowang@pku.edu.cn; wj-iao@mail.iggcas.ac.cn

Orogens are major sites for crustal growth on Earth. They record a unique formation and evolutionary history of the continental crust that distinguishes Earth from other planets. Therefore, orogenesis and crustal growth, and particularly their relationships, are fundamental issues in the Earth sciences.

Orogens are characterized and categorized using a range of features, leading to the identification of convergent and extensional or small-cold and large-hot orogens[1,2], the external and internal orogenic systems[3], and Alpine-, Himalayan-, and Turkic-type collisional orogenic belts[4]. They are commonly grouped into collisional, accretionary, or intracratonic[5–9].

However, orogens are mostly composite and experience multiple stages of the orogenic processes, such as the accretion of relatively small terranes (or soft collision) and continental collision, and these orogens are commonly called composite orogens[4,8,10], Thus, orogens vary in their nature and style, defining a broad spectrum of types that encompass the Wilson Cycle[11]. There are a lack of robust ways or methods to quantitatively characterize, define, and/or classify the various types of orogens (particularly composite orogens), although some previous studies have sought to compare accretionary orogens based on terrane longevity, accretion rates, and juvenile crust production[4–6,12]. Every orogen contains a distinct complex history, which also makes the comparison with other orogens very difficult. Seeking a way or method to objectively and quantitatively characterize and/or classify orogens based on their final compositional architecture and crustal growth patterns (or stages) is crucial.

In this paper, we applied Nd isotope mapping as a "Big Data" approach to evaluating the compositional architecture and crustal growth patterns of the eight well-studied Phanerozoic orogens to provide a semi-quantitative basis for comparison. Specifically, the areal proportion of primitive/juvenile to evolved/reworked crust has been used as a semi-quantitative criterion to characterize the crustal compositional architecture and evolution of orogens. This study provides insights into the relationships between orogenesis and crustal growth.

Results

Representative and well-studied orogens. Two end-members of orogens have been commonly proposed: accretionary and collisional[5,6,8,9]. Accretionary orogens form by the accretion of diverse components (e.g., dominantly oceanic components including island arcs, ophiolites, and fragments of oceanic plateaus and microcratons) accreted from the downgoing plate and eroded from the upper plate at active oceanic subduction zones, whereas collisional orogens form as continental plates are progressively subducted[5,8,13]. Most accretionary orogens now occur as "fossil" orogenic belts within and/or at the margins of consolidated continents[14]. Phanerozoic accretionary and collisional examples include the eight orogens discussed below (Fig. 1 and Supplementary Note 1).

The Altaids, or Altaid tectonic collage[4,15], or the southern Central Asian Orogenic Belt (CAOB)[16,17], is located between the Siberian, Baltic, and Tarim-North China cratons (Fig. 1). It records protracted accretion of the Paleo-Asian Ocean and subsequent collision of ancient terranes from 1000 (mainly 650) to 220 Ma[12,17,18]. followed by the accretion and closure of the Mongol-Okhotsk Ocean from 300 to 150 Ma[4,12,15,17–19]. The Altaids is generally considered to be the world's largest accretionary orogen and the important site of considerable Phanerozoic continental growth[12,16–18]. The Appalachian Orogen in North America was formed by accretion and/or soft collision of several juvenile terranes and ancient crustal blocks and the terminal continent-continent amalgamation of Laurentia and Gondwana in the Permian[10,20]. One of the best-exposed cross-sections through the orogen is exposed in Newfoundland[10]. The North American Cordillera is considered to be an archetypal accretionary orogen[5,7]. The major accretionary processes occurred during the Mesozoic, although evidence exists that subduction began ~420 Ma ago[21,22]. The Lachlan Orogen is part of the Paleozoic Tasman Orogenic system of eastern Australia and Gondwana[23]. The orogen formed during the stepwise closure (500–340 Ma) of sequential oceanic back-arc basins formed behind a long-lived, outboard migrating subduction zone that is preserved in the New England Fold Belt[23].

The following four representative and well-studied Phanerozoic collisional orogens are investigated here (Supplementary Note 1). The Caledonian Orogen or Caledonides formed during the Silurian collision between Laurentia and Baltica[24]. The Variscan Orogen or Variscides was the result of the late Paleozoic collision between Gondwana and Laurussia[25]. The Qinling-Dabie Orogen initially formed during the closure of the Proto-Tethyan Ocean and finally due to the closure of the Paleo-Tethyan oceans and the early Mesozoic collision between the North China Craton and South China Craton[26]. The Tethyan Tibetan Orogen (i.e., the Tibetan Plateau) experienced Mesozoic accretion–collision of terranes following the closure of the Proto- and Paleo-Tethyan Oceans, and the final Cenozoic (60–50 Ma) India–Eurasia collision during the closure of the Neo-Tethys Ocean[27,28].

Isotopic mapping of the eight orogens. We used felsic and intermediate igneous rocks (as classified in the original literature, see Supplementary Note 1) to undertake Nd isotope mapping and then to investigate the compositional architecture and crustal growth patterns, i.e., the final result of preservation of long-term crustal growth formed during (accretionary and collisional) orogenesis. Felsic igneous rocks (e.g., granitoids) are generally derived from the crust and their isotope features commonly reflect the basement rocks of the crust. Some intermediate igneous rocks may be produced by fractional crystallization of mantle-derived mafic magmas, but many are considered hybrids generated by magma mixing or contamination, as indicated by consistently old (Nd and Hf) model ages relative to emplacement age. Thus, we assumed that their isotopic features represent the overall, mixed characteristics of the deep crust. More importantly, we selected these felsic and intermediate igneous rocks to ensure a broad range of rock types within each orogen, which increased the number of isotopic analyses to make the comparisons more credible and reduce statistical uncertainties. Data were collected from the literature and websites. The data are reliable according to the sources, which was confirmed by the good linear correlation of their $\varepsilon_{Nd(t)}$ values vs. two-stage Nd depleted mantle model ages (T_{DM2}; Supplementary Note 2).

We conducted whole-rock Nd isotope mapping (methods in Supplementary Note 3) using the compiled datasets of 9332 Sm-Nd data with ages, including 240 new analyses, i.e., 71 from the Appalachian (Newfoundland) orogen and 169 from the Altaids (Supplementary Data 1-8). The isotopic maps cover all outcrop areas of a whole orogen such as the Altaids (~7,010,625 km^2), North American Cordillera (~6,693,675 km^2), Newfoundland Appalachians (~115,236 km^2), Lachlan (532,550 km^2), Tethyan Tibet (~2,403,600 km^2), Variscan (~1,237,600 km^2), and the Qinling-Dabie (~294,075 km^2) orogens. For the Caledonian orogen that has been split by the Atlantic Ocean opening, the mapped areas (~666,800 km^2) cover most of the outcrop areas of the orogen, including the British, Scandinavian, Svalbard, and Greenland regions (Fig. 2).

Nd isotope parameters, specifically $\varepsilon_{Nd}(t)$ values and two-stage model ages (T_{DM2}, Ga), are shown as contour maps in Fig. 2 and

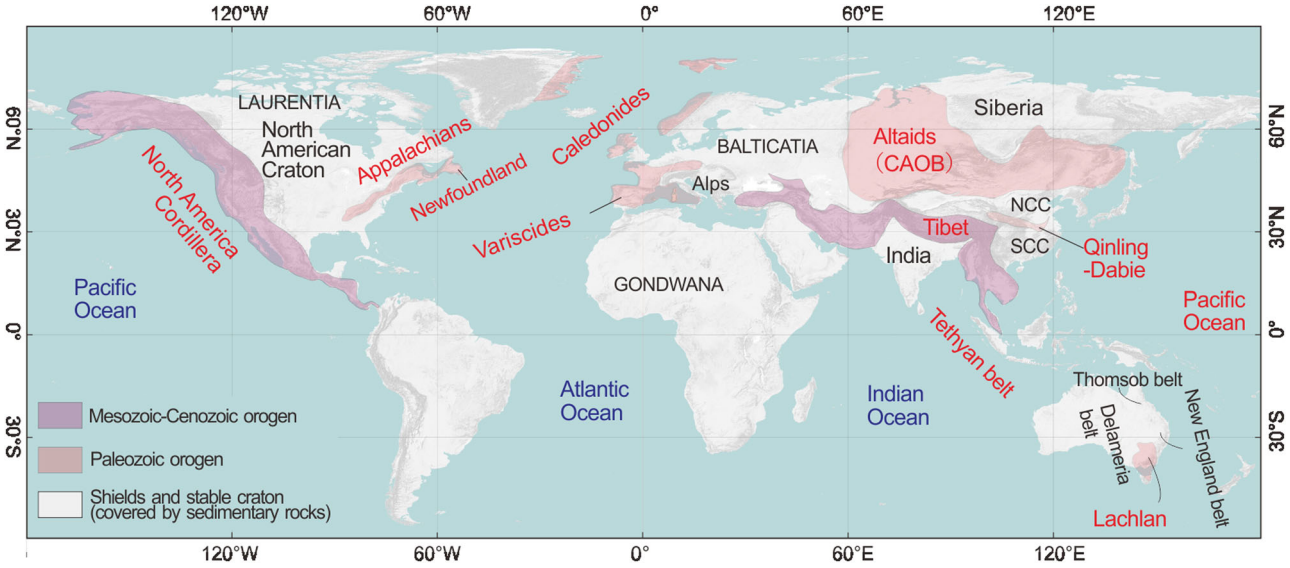

Fig. 1 A map of the eight representative and well-studied orogens in the world, showing their locations and tectonic background. NCC North China Craton; SCC South China Craton. The digit topographic map comes from https://services.arcgisonline.com.

Supplementary Note 2. These maps demonstrate the distribution of isotopic domains and their areal extent (Supplementary Data 9). The domains are defined by per 2 $\varepsilon_{Nd}(t)$ value interval and shown in Fig. 2 by 15 different color zones (Fig. 2). These domains can be grouped into six isotopic provinces (Supplementary Data 10): (I) extremely or highly primitive (i.e., juvenile), characterized by $\varepsilon_{Nd}(t)$ value > +6 and young Nd mode ages (T_{DM2} < 0.4 Ga); (II) moderately primitive by $\varepsilon_{Nd}(t)$ = +4 to +6, relatively young T_{DM2} values (0.4–0.8 Ga); (III) slightly primitive by $\varepsilon_{Nd}(t)$ value = +4 to 0, T_{DM2} = 0.8–1.0 Ga; (IV) slightly evolved, by $\varepsilon_{Nd}(t)$ = −4 to 0, T_{DM2} = 1.0–1.2 Ga; (V) moderately evolved, by $\varepsilon_{Nd}(t)$ = −10 to −4, T_{DM2} = 1.2–1.6 Ga; (VI) highly evolved provinces, by $\varepsilon_{Nd}(t)$ <−10, T_{DM2} = 1.6–2.8 Ga.

These isotopic domains reflect the distributions of isotopic signatures of the source rocks in the basement. Effectively, the approach is "basement terrane mapping". Accordingly, we denote juvenile versus reworked crust and place constraints on the compositional architecture. The juvenile crust is generally defined by positive $\varepsilon_{Nd}(t)$ values (>0), which are commonly used (e.g., refs. [5,6]). The juvenile crust in the isotopic maps is characterized by provinces I to III. Correspondingly, the reworked crust is defined by negative $\varepsilon_{Nd}(t)$ value (<0), characterized by provinces IV to VI.

From these maps, we obtain the relative areal proportions of primitive and evolved isotopic compositions and can determine juvenile and reworked crustal provinces, respectively (Figs. 2 and 3 and Supplementary Data 9). The juvenile areal proportions of the Altaids, North American Cordillera, Newfoundland Appalachians, Lachlan, Tethyan Tibet, Caledonides, Variscides, and the Qinling-Dabie Orogen are ~58%, ~54%, ~40%, ~31%, ~3%, ~1%, ~1%, and 1 < % of total areas of each orogen, respectively, quantitatively evaluating the degree of preservation of crustal growth (Fig. 3). The percentages were calculated from the areas of the isotopic provinces or domains and their precision depends on the numbers of isotopic data and their homogeneity in distribution (Fig. 2). With increasing data, the isotopic mapping may be more precise, but the percentage results may be approximately similar.

Figure 4 shows types of crustal growth curves. These curves reflect the percentages of the areas of $\varepsilon_{Nd}(t)$ and T_{DM2} isotopic domains (Fig. 3 and Supplementary Data 10), so they directly denote crustal growth, which is different from commonly used crustal growth curves made by cumulative frequency plots of global isotopic datasets[29–34]. The curves of the four accretionary orogens (Altaids, North American Cordillera, Newfoundland Appalachians, and Lachlan) all extend to the right side (more positive $\varepsilon_{Nd}(t)$ and young T_{DM2}) compared with other curves (Fig. 4), demonstrating these accretionary orogens contain more (>30%) juvenile crust. Among them, the Altaids hosts the highest accumulation and/or percentage of juvenile crust, followed by the North American Cordillera, Newfoundland Appalachians, and the Lachlan Orogens, with the Tethyan Tibet, Caledonides, Variscides, and the Qinling-Dabie Orogens having the least amount of juvenile crust. Clearly, the accretionary orogens contain much larger volumes of juvenile crust than the collisional orogens (Figs. 2–4), quantitatively confirming that accretionary orogens are primary sites of juvenile continental crust production, as many previous studies show[5,13,35,36].

Our Nd isotope mapping results are consistent with those of zircon Hf isotope mapping and xenocryst studies of some orogens, such as in the Altai–Junggar–Tianshan region of the southern Altaids[37–39], the Qinling-Dabie[40], and the Tethyan Tibet[28]. In the Altai–Junggar region, Hf isotopic mapping of the Palaeozoic granitoids indicated a sharp contrast between the deep crustal compositions of the Altai and Junggar regions: the reworked (ancient) crust in the central Altai and juvenile in the Junggar[38]. This is consistent with the result of our Nd isotopic mapping (Fig. 2a). The isotopic mapping results are also consistent with geophysical investigations[41]. For example, primitive isotopic domains (province I; Supplementary Data 10) reveal the existence of deep-seated highly juvenile crust in the western Junggar of the Altaids. Similarly, magnetotelluric imaging also revealed this deep-seated Paleozoic paleo-oceanic crust[42]. Furthermore, shear wave (Vs) seismic tomography at depths of 30–40 km, based on >200 stations, identified a high-velocity body in the western Junggar orogen, and low-velocity bodies in the Altai and Tianshan mountains[41]. These coincide with provinces I and II in the western Junggar orogen and evolved Provinces V and IV in the Tianshan and Altai mountains.

Compositional architecture (crustal patterns) of the eight orogens. The proportions of juvenile to reworked crust contrast between the orogens. The Altaids contains a large area of juvenile crust accounting for ~ 4,107,350 km^2 and ~58% area (Figs. 2 and 3 and Supplementary Data 9 and 10). Considering (1) the Altaids is an (extensional) accretionary orogen that preserves significant

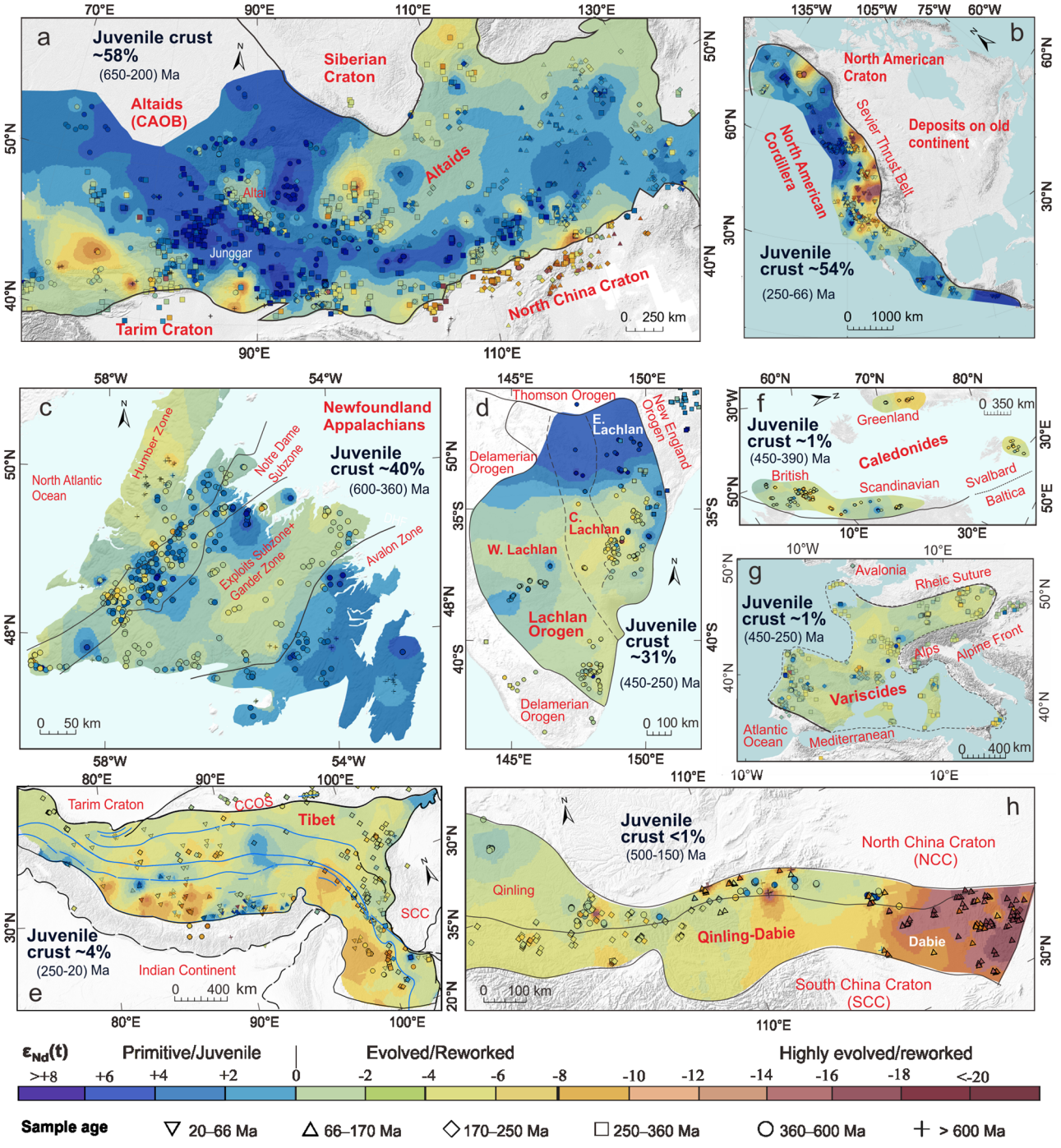

Fig. 2 $\varepsilon_{Nd}(t)$ contour maps of the eight orogens, showing spatial variations of $\varepsilon_{Nd}(t)$ values and distribution of Nd isotopic domains. a Altaids, **b** North American Cordillera, **c** Newfoundland Appalachians, **d** Lachlan, **e** Tethyan Tibet, **f** Caledonides, **g** Variscides, and **h** Qinling-Dabie orogens, showing spatial variations of $\varepsilon_{Nd}(t)$ values and distribution of Nd isotopic domains. The lower row legend shows the colors expressed as variations in $\varepsilon_{Nd}(t)$ values. E. = Eastern; C. = Central; W. = Western. See the explanations and uncertainties in the text and dataset in Supplementary Data 1–8. The digit topographic map comes from https://services.arcgisonline.com.

amounts of oceanic crust, accretionary wedges, and other juvenile tectonic terranes; and (2) there are few significant over-thrusts (different from the Tethyan Tibit and Qinling-Danie orogen), we assume that the deep-seated juvenile crust largely represents the whole crust. Then we estimate the juvenile crust in the Altaids as a volume of ~184,830,750 km^3, using the total areas of isotopic mapping (~7,010,375 km^2) and a 40–50 km (an average of 45 km) crustal thickness[43]. Accordingly, the Altaids hosts both the highest percentage (~58%) and the largest volume of juvenile crust among the eight orogens. Comparably, the North American Cordillera (~54%), Newfoundland Appalachians (~40%), and the Lachlan (~31%) contain less juvenile crust and more evolved crust, similar to the complex accretionary orogens defined by Condie[6]. These are consistent with their geological characteristics. For instance, the Newfoundland Appalachian was subjected to the successive accretion of Gondwana-derived terranes with an older pre-orogenic history of crustal formation, interspersed with oceanic fragments[10]. The Paleozoic Lachlan Orogen acquired its transitional character by

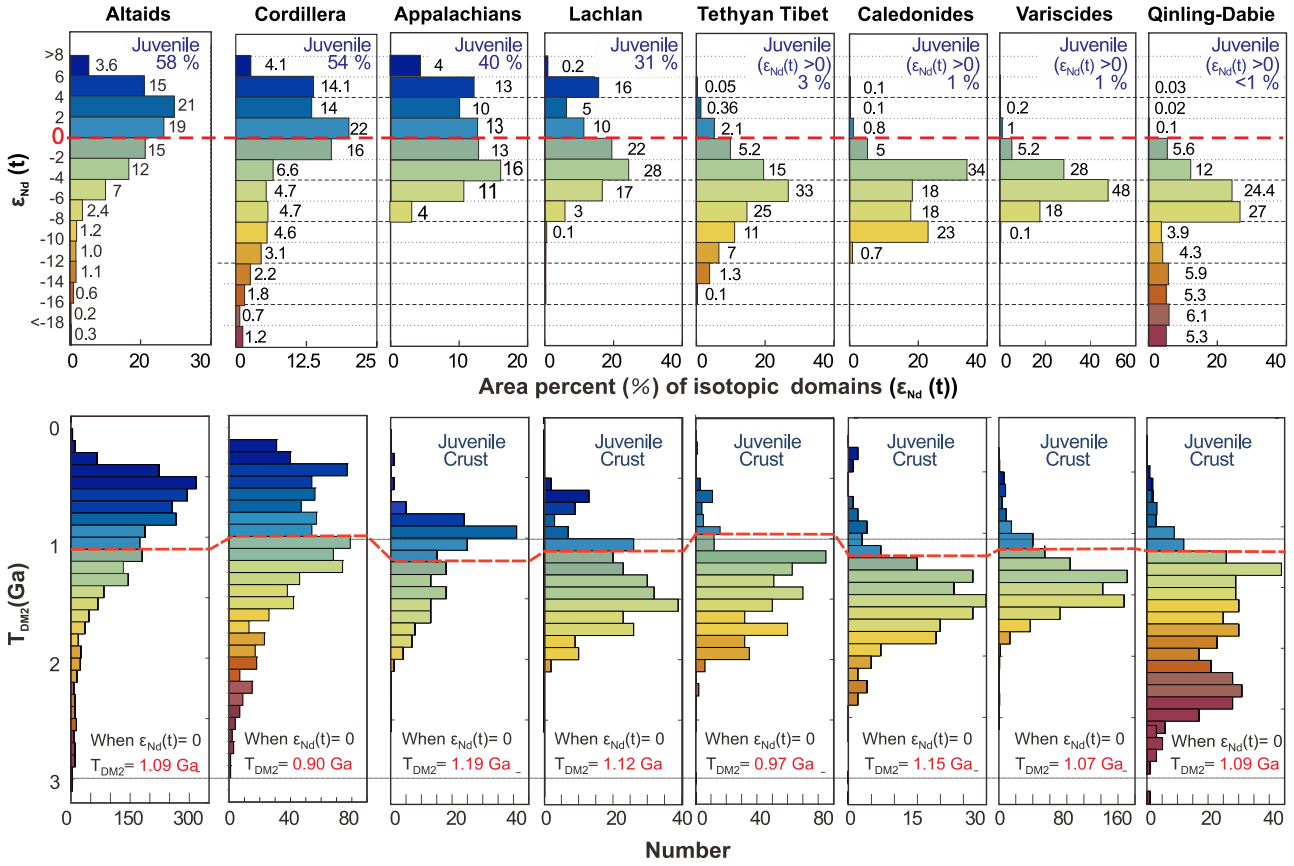

Fig. 3 Diagrams of $\varepsilon_{Nd}(t)$ value vs. area percent of isotopic domains (upper row), showing the total areal percent of the primitive province or juvenile crust ($\varepsilon_{Nd}(t) > 0$; blue area) for each orogen. The color scales are defined by per 2 $\varepsilon_{Nd(t)}$ value interval, the same as those in Fig. 2. The lower row diagrams are histograms of T_{DM2} for each orogen. Blue areas denote primitive domains or juvenile crust younger than T_{DM2} corresponding to $\varepsilon_{Nd}(t) = 0$; whereas the warmer colors reflect increasing amounts of ancient crust. The color scales are defined by per 200 Myr T_{DM2} interval, the same as those in Supplementary Fig. 2. All the data are listed in Supplementary Data 9 and 10.

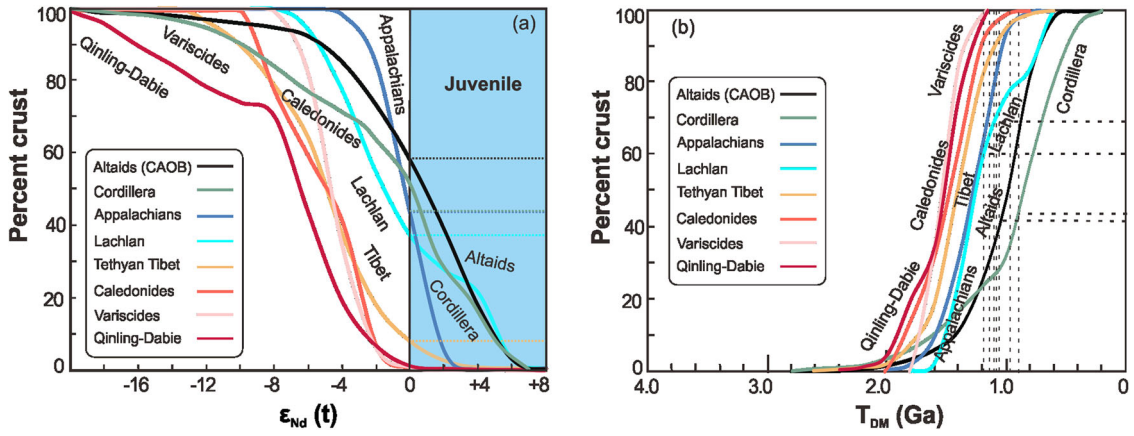

Fig. 4 Crustal growth curves for the eight orogens. The curves show **a** the percentage areas of crust produced per two $\varepsilon_{Nd}(t)$ value intervals and **b** per 200 Myr T_{DM2} interval. The percentages are drawn from the areas of $\varepsilon_{Nd}(t)$ and T_{DM2} isotopic domains respectively (Fig. 3 and Supplementary Data 10). So, these crustal growth curves directly denote crustal growth, which is different from commonly used crustal growth curves made by cumulative frequency plots of global isotopic datasets[29–34]. The vertical dashed lines (b) represent T_{DM2} corresponding to $\varepsilon_{Nd}(t) = 0$, and the dotted horizontal lines denote the percentages of the crust when $\varepsilon_{Nd}(t) = 0$, the distinction between juvenile and evolved. Taking the Altaids for instance, ~58% of juvenile crust had been generated at ~1.0 Ga. The colors of the solid and dotted lines represent different orogens. Data are listed in Supplementary Data 9.

the deposition of cratonic (Proterozoic) sediments into sequentially formed backarc basins and the sediments were progressively buried and melted during various stages of orogeny to produce S-type granites[35]. Elsewhere in the orogen, the juvenile meta-igneous crust was melted to produce I-type granites.

In contrast, the above four collisional orogens, located on the left sides of the curves (Fig. 4), contain much less juvenile (or much larger reworked) crust (Fig. 2). The Qinling-Dabie Orogen contains not only the least (<1%) juvenile crust (or the largest reworked crust) but also the most ancient crust

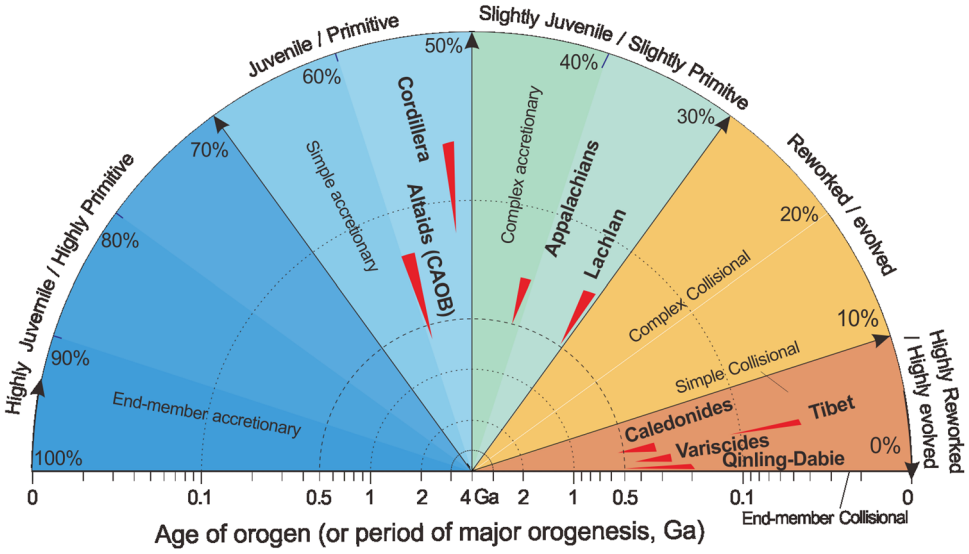

Fig. 5 A hemispheric diagram showing the classification and characteristics of orogens in terms of their compositional architecture (areal percent of juvenile compositions) and ages of orogens. Sectors represent a continuous transition from highly primitive (juvenile crust 100%) to highly evolved (juvenile crust ~0%) compositions. Concentric semi-circles with logarithmic coordinates denote the age range of the orogens (such as 500–340 Ma for the Lachlan Orogen).

($\varepsilon_{Nd}(t)$ <−16; Figs. 3 and 4). This is consistent with the orogen's character that the South China Craton was overridden by the dominantly Archean North China Craton (deep continental subduction) as indicated by the continental ultra-high-pressure metamorphism[44].

Discussion

From the above, we propose an approach to divide the orogens, based on the areal proportions of juvenile (primitive) or reworked crust, into dominantly juvenile (primitive isotope values) and reworked (evolved isotope values) types (Fig. 5). We propose that an orogen can be placed into six categories, based on its composition and timing of orogeny (Fig. 5).

Previous studies demonstrated that orogens are mostly composite and evolve with time, and most accretionary orogens end up in a collisional phase (e.g.[45],). It is potentially difficult to distinguish between accretionary and collisional orogens in practice; even the two "terms" are inconsistently understood by different authors. For instance, the Altaids, a typical accretionary orogen[12,17,18], still hosts collisional features and has been called a Turkic-type collisional orogenic belt[4]. The Appalachian orogen is also viewed as a collisional orogen[5]. The Variscides is generally considered to be a collisional orogen[25], but is still considered to be accretionary prior to collision (e.g.,[5,*pp149*]). Condie[5,6] further divided accretionary orogens into simple (chiefly juvenile terranes with lifespans of <100 m.y.) and complex (with both juvenile accreted, components and exotic microcratons, with terrane lifespans of ≥100 m.y.) types. Our characterization and classification of orogens enable us to objectively and semi-quantitatively contrast between them (Fig. 5). Orogens with juvenile crust between 70–50% correspond to simple (typical) accretionary (e.g., the Altaids, ~58%), and 50–30% to complex accretionary (e.g., North American Cordillera (~54%), Newfoundland Appalachians (~40%), Lachlan Orogen (~31%)). Furthermore, we consider orogens with 30–10% juvenile component as complex collisional (which contains more juvenile crust than typical collisional and can be viewed as falling in between accretionary and collisional), 10–1% as simple (or typical) collisional (e.g., Tethyan Tibet (~3%), Caledonides (~1%), and Variscides (~1%)). Typical oceanic arcs containing >70% juvenile crust and collisional orogens with <1% juvenile crust (e.g., the Qinling-Dabie Orogen) may be regarded as the end members of the entire orogenic array, and the formers may be preserved in an accretionary orogenic system. Oceanic arcs built on continental ribbons may vary between endmember and simple accretionary orogens depending on the proportion of the old basement. We predict New Zealand and Japan would fit the simple accretionary category. This study provides a semi-quantitative approach to characterizing orogen types.

It is important to further distinguish the collisional and accretionary phases of an orogen and to compare the evolutionary phase of an orogen with a similar phase in another orogen, if possible. Figures 2 and 3 show the percentage area of primitive and/or evolved isotopic domains and the crustal growth curves of the eight orogens. These provide a quantitative comparison of the amount of juvenile and reworked crust of these orogens in different phases, but it is difficult to distinguish the accretionary (juvenile) and collisional (reworked) phases for one orogen and to compare the orogen with a similar phase in another orogen. As an example, we produced isotopic maps for the syn-accretionary (600–320 Ma) and post-accretionary or collisional (320–150 Ma) igneous rocks in the Altaids[41], which assumes collision occurred at 320 Ma. However, some authors suggest final closure of the major intervening (Paleo-Asian) ocean occurred in the Permian or Triassic. Assuming 320 Ma collision, the results show that the accretionary phase contributed ~3,156,900 km^2 of the juvenile crust, accounting for ~45 % of the surface area of the Altaids (all isotopic provinces), and the collision (320–150 Ma) ~950,450 km^2, accounting for ~14%. They may be considered to be representatives of the earlier accretionary and latter collisional phases, respectively.

In general, it is not easy to identify and date an accretionary and a collisional phase, particularly if the collisional process was diachronous, where both phases of orogeny involved a long-lasting terminal orogenic process (e.g., the Altaids and Appalachians). Similarly, if the accretionary orogen underwent repeated extension-contraction phases, some syn-accretionary granites might be regarded as "post-collisional". For example, many S-type granites in the Lachlan orogen are called "post-collisional" (e.g., ref. [46]), but most are Silurian and accretion

continued until the Middle-Late Devonian following a significant Early Devonian extension phase. Therefore, this study mainly focuses on a comparison of the overall architecture formed during all major syn-orogenic (accretionary and collisional) processes, which is achieved by a comparison study of similar igneous rock types that formed during the major orogenic (accretionary and collisional) processes. Although it would be better to compare the similar phases of the evolution of the complete lifetime of an orogen if there were sufficient data, the present work establishes a first-order difference between accretionary and collisional orogens.

From the point of view of the Wilson Cycle, orogens begin as accretionary and evolve into collisional, culminating in the termination phase during supercontinent amalgamation[6,9,11]. Thus, each orogen may be viewed as having reached a certain stage of its evolution path in the Wilson Cycle. Moreover, active accretionary orogens will continue to evolve; for instance, the active accretionary orogenic systems around the margins of the Pacific Ocean, such as the North and South American Cordillera, may evolve or be reformed into collisional or even intracratonic orogens if the Pacific Ocean closes in the future (e.g., ref. [47]). Based on this expected orogenic evolution, we can use the decrease in the juvenile crustal areal proportions to semi-quantitatively trace the orogenic stages from accretion to collision as each orogen progresses through the Wilson Cycle (Fig. 5).

This study also marks strong links between orogenesis and crustal growth. Crustal growth is defined as the addition of mantle-derived material to the crust, and rates are usually based on cumulative frequency plots of global isotopic data[29–34]. However, there are many unconstrained aspects of the statistical treatment of data (such as data size and their homogeneous distribution), and such global compilations do not reflect the relationship between orogenesis and crustal growth. Here we have applied areal proportions of juvenile crust determined by isotopic mapping to individual orogens to show which have contributed significantly to crustal growth and which have not.

The Altaids was regarded as the best example of Neoproterozoic-Phanerozoic continental growth[15,16,48]. However, this has been questioned recently, where it is argued that no unusual continental growth occurred at this time[49]. Our study indicates that the Altaids contains both the largest volume and highest proportion of juvenile crust (see above) and much of it formed during the Neoproterozoic-Phanerozoic (Figs. 2–4). Accordingly, the Altaids can be viewed as a "fossil" of the largest Phanerozoic crustal growth area in orogens worldwide[41] and it serves as the best example of Phanerozoic accretion and crustal growth to compare with the Archean Cratons to test for similarities or differences in the formation of continents through time[50]. Additionally, our datasets can be used to confirm the onset of accretionary orogenic systems and plate tectonics in the Archean Eon. Our study helps to untangle the mystery of whether or not significant continental crustal growth occurs during orogenesis, including the Phanerozoic orogenesis[16,29,31,33,34].

Untangling the mystery of crustal growth and its mechanisms is an interesting and fundamental issue in the Earth sciences. Several mechanisms have been invoked for the generation of juvenile crust during (Phanerozoic) subduction/accretion[5,6,31,51,52]. Accretion, particularly extensional accretion, is beneficial for the generation of juvenile crust[5,6,8,9], which is produced by the melting of a mantle wedge metasomatized by subducted fluids, by melting of subducted oceanic crust, or by rapid remelting of basaltic underplates at the base of arcs (e.g., ref. [52]). Some researchers (e.g., ref. [51]) suggested that collisional orogens (or collision zones) are primary sites not only for continental crustal growth but also for net continental crustal growth (e.g., the Tethyan Tibet), and the juvenile crust (syncollisional andesites) are isotopically dominated by mantle signatures inherited from ocean crust that was derived from the mantle at mid-ocean ridges or derived from mantle-derived magmas generated during break-off or delamination in a post-collisional setting (e.g., ref. [28]). The crustal growth estimated by the isotopic mapping is observed as preservation of juvenile crust; so, it is net growth. Our Nd isotopic mapping confirms the observations (e.g., ref. [45]) that a large amount (30–60%) of juvenile crust occurs in accretionary orogens, but less (<5%) juvenile crust occurs in collisional orogens (Fig. 5) and provides a quantitative amount and proportion of juvenile crust.

Preservation is important for net crustal growth. Oroclines and soft collision may provide good conditions for the preservation of juvenile crust, such as a large number of oroclines in the Altaids[4,18,19]. Numerous oroclines with different sizes have been identified in the Altaids[15,18,19]. These oroclines contain many trapped structures, e.g., the trapped structures in the Junggar region of the western Altaids, and these structures preserve a large proportion of the oceanic crustal systems and other types of juvenile continental crust. Additionally, soft collision facilitates the preservation of accretionary terranes and suture zones dominated by juvenile crust. These soft collision zones are typical of accretionary orogens and are distinct from the hard collision events of collisional orogens that may result in the removal of the juvenile crust by crustal-scale thrusting and subsequent erosion or by deep subduction of continental crust.

In summary, the crustal pattern or compositional architecture of an orogen reflects both the production and preservation of juvenile crust. Delineation of the compositional architecture and crustal patterns by isotope mapping allows objective and quantitative characterization and classification of orogens, obtaining an indelible imprint that relates to the areal proportion of juvenile crust preserved in the system. Accordingly, we can unveil the relationships between orogenesis and crustal growth, providing an alternative approach for constraining the evolution of Earth. We provide an innovative way to directly compare different complex orogens and divide the orogens into different evolution stages through isotope mapping and estimating percentages of areas (volume) of juvenile crust quantitatively.

Methods

We used the chondritic values $(^{143}Nd/^{144}Nd)_{CHUR} = 0.512638$ and $(^{147}Sm/^{144}Nd)_{CHUR} = 0.1967$[53] to calculate all Nd data (Fig. 2) and to obtain $\varepsilon_{Nd}(t)$ values and Nd depleted mantle model ages (one-stage, T_{DM1}, and two-stage T_{DM2}; Supplementary Note 2). The juvenile crust is defined as having positive $\varepsilon_{Nd}(t)$ values (i.e., >0)[54].

Neodymium and model age contour maps were produced in two steps. Firstly, we used the inverse distance weighted interpolation method and Surfer v.13.0 software for gridding. Given the uneven distribution of the isotope datasets, we sequentially used two spacings and searched radii (i.e., 50–500 and 5–100 km, respectively) for the gridding. Secondly, we converted the grid data to *.img format in ArcGIS, reclassified the data into equal intervals and then produced the contour maps with Spatial Analyst Tools. The obtained and compiled data, data sources, and analytical methods are presented in Supplementary Data 1–8 and Supplementary Note 3.

Data availability

Supplementary Data are available in Figshare data repository under https://doi.org/10.6084/m9.figshare.22345072.v1.

Received: 23 August 2022; Accepted: 28 March 2023;
Published online: 10 April 2023

References

1. Collins, W. J. Hot orogens, tectonic switching, and creation of continental crust. *Geology* **30**, 535–538 (2002).
2. Jamieson, R. A. & Beaumont, C. On the origin of orogens. *GSA Bull.* **125**, 1671–1702 (2013).

3. Collins, W. J., Belousova, E. A., Kemp, A. I. S. & Murphy, J. B. Two contrasting Phanerozoic orogenic systems revealed by hafnium isotope data. *Nat. Geosci.* **4**, 333–337 (2011).
4. Şengör, A. M. C., Natal'in, B. A., Sunal, G. & Voo, Rvander The tectonics of the Altaids: crustal growth during the construction of the continental lithosphere of Central Asia between ~750 and ~130 Ma Ago. *Annu. Rev. Earth Planet. Sci.* **46**, 439–494 (2018).
5. Condie, K. C. in *4-D Framework of Continental Crust* (eds Hatcher, R. D., Jr., Carlson, M. P., McBride, J. H. & Martínez Catalán, J. R.) 145–158 (Geological Society of America, 2007).
6. Condie, K. Preservation and recycling of crust during accretionary and collisional phases of proterozoic orogens: a bumpy road from Nuna to Rodinia. *Geosciences* **3**, 240–261 (2013).
7. Coney, P. J., Jones, D. L. & Monger, J. W. H. Cordilleran suspect terranes. *Nature* **288**, 329–333 (1980).
8. Cawood, P. A. et al. Accretionary orogens through Earth history. *Geol. Soc. Lond. Spec. Publ.* **318**, 1–36 (2009).
9. Cawood, P. A., Strachan, R. A., Pisarevsky, S. A., Gladkochub, D. P. & Murphy, J. B. Linking collisional and accretionary orogens during Rodinia assembly and breakup: implications for models of supercontinent cycles. *Earth Planet. Sci. Lett.* **449**, 118–126 (2016).
10. van Staal, C. R. & Zagorevski, A. Accretion, soft, and hard collision: similarities, differences and an application from the Newfoundland Appalachian Orogen. *Geosci. Canada* **47**, 103–118 (2020).
11. Wilson, R. W., Houseman, G. A., Buiter, S. J. H., McCaffrey, K. J. W. & Doré, A. G. Fifty years of the Wilson Cycle concept in plate tectonics: an overview. *Geol. Soc. Lond. Spec. Publ.* **470**, 1–17 (2019).
12. Xiao, W. J. et al. A tale of amalgamation of three collage systems in the Permian-Middle Triassic in Central Asia: Oroclines, sutures and terminal accretion. *Annu. Rev. Earth Planet. Sci.* **43**, 477–507 (2015).
13. DeCelles, P. G., Ducea, M. N., Kapp, P. & Zandt, G. Cyclicity in Cordilleran orogenic systems. *Nat. Geosci.* **2**, 251–257 (2009).
14. Scholl, D. W. & Von Huene, R. Implications of estimated magmatic additions and recycling losses at the subduction zones of accretionary (non-collisional) and collisional (suturing) orogens. *Geol. Soc. Lond. Spec. Publ.* **318**, 105–125 (2009).
15. Sengör, A. M. C., Natal'in, B. A. & Burtman, V. S. Evolution of the Altaid tectonic collage and Palaeozoic crustal growth in Eurasia. *Nature* **364**, 299–307 (1993).
16. Jahn, B. M., Wu, F. Y. & Chen, B. Granitoids of the Central Asian Orogenic Belt and continental growth in the Phanerozoic. *Trans. R. Soc. Edinb. Earth Sci.* **91**, 181–193 (2000).
17. Windley, B. F., Alexeiev, D., Xiao, W., Kroner, A. & Badarch, G. Tectonic models for accretion of the Central Asian Orogenic Belt. *J. Geol. Soc. Lond.* **164**, 31–47 (2007).
18. Xiao, W. J. et al. Late Paleozoic to early Triassic multiple roll-back and oroclinal bending of the Mongolia collage in Central Asia. *Earth Sci. Rev.* **186**, 94–128 (2018).
19. Wang, T. et al. Rollback, scissor-like closure of the Mongol-Okhotsk Ocean and formation of an orocline: magmatic migration based on a large archive of age-data. *Natl Sci. Rev.* **9**, nwab210 (2022).
20. Williams, H. Appalachian Orogen in Canada. *Can. J. Earth Sci.* **16**, 792–807 (1979).
21. Chapman, J. B., Runyon, S. E., Shields, J. E., Lawler, B. L. & Haxel, G. B. The north American cordilleran anatectic belt. *Earth Sci. Rev.* **215**, 103576 (2021).
22. Monger, J. W. H., Price, R. A. & Templeman-Kluit, D. J. Tectonic accretion and the origin of the two major metamorphic and tectonic welts in the Canadian Cordillera. *Geology* **10**, 70–75 (1982).
23. Foster, D. A., Gray, D. R., Spaggiari, C., Kamenov, G. & Bierlein, F. P. Palaeozoic Lachlan Orogen, Australia; accretion and construction of continental crust in a marginal ocean setting: Isotopic evidence from Cambrian metavolcanic rocks. *Geol. Soc. Lond. Spec. Publ.* **318**, 329–349 (2009).
24. Dewey, J. F. & Strachan, R. A. Changing Silurian–Devonian relative plate motion in the Caledonides: sinistral transpression to sinistral transtension. *J. Geol. Soc. Lond.* **160**, 219–229 (2003).
25. Matte, P. The Variscan collage and orogeny (480–290 Ma) and the tectonic definition of the Armorica microplate: a review. *Terra Nova* **13**, 122–128 (2001).
26. Dong, Y. & Santosh, M. Tectonic architecture and multiple orogeny of the Qinling Orogenic Belt, Central China. *Gondwana Res.* **29**, 1–40 (2016).
27. Van Hinsbergen, D. J. et al. Greater India Basin hypothesis and a two-stage Cenozoic collision between India and Asia. *Proc. Natl Acad. Sci. USA* **109**, 7659–7664 (2012).
28. Hou, Z. Q. et al. Lithospheric architecture of the Lhasa Terrane and its control on ore deposits in the Himalayan-Tibetan Orogen. *Econ. Geol.* **110**, 1541–1575 (2015).
29. Reymer, A. & Schubert, G. Phanerozoic addition rates to the continental crust and crustal growth. *Tectonics* **3**, 63–77 (1984).
30. Belousova, E. A. et al. The growth of the continental crust: constraints from zircon Hf-isotope data. *Lithos* **119**, 457–466 (2010).
31. Hawkesworth, C., Cawood, P. & Dhuime, B. Continental growth and the crustal record. *Tectonophysics* **609**, 651–666 (2013).
32. Dhuime, B., Wuestefeld, A. & Hawkesworth, C. J. Emergence of modern continental crust about 3 billion years ago. *Nat. Geosci.* **8**, 552–555 (2015).
33. Dhuime, B., Hawkesworth, C., Delavault, H. & Cawood, C. Rates of generation and destruction of the continental crust: implications for continental growth. *Phil. Trans. R. Soc. A* **376**, 20170403 (2018).
34. Spencer, C. J., Roberts, N. M. W. & Santosh, M. Growth, destruction, and preservation of Earth continental crust. *Earth Sci. Rev.* **172**, 87–106 (2017).
35. Kemp, A. I. S., Hawkesworth, C. J., Collins, W. J., Gray, C. M. & Blevin, P. L. Isotopic evidence for rapid continental growth in an extensional accretionary orogen: the Tasmanides, eastern Australia. *Earth Planet. Sci. Lett.* **284**, 455–466 (2009).
36. Naeraa, T. et al. Hafnium isotope evidence for a transition in the dynamics of continental growth 3.2 Gyr ago. *Nature* **485**, 627–630 (2012).
37. Wang, T. et al. Nd–Sr isotopic mapping of the Chinese Altai and implications for continental growth in the Central Asian Orogenic Belt. *Lithos* **110**, 359–372 (2009).
38. Song, P. et al. Contrasting deep crustal compositions between the Altai and East Junggar orogens, SW Central Asian Orogenic Belt: Evidence from zircon Hf isotopic mapping. *Lithos* **328–329**, 297–311 (2019).
39. Huang, H. et al. Rejuvenation of ancient micro-continents during accretionary orogenesis: Insights from the Yili Block and adjacent regions of the SW Central Asian Orogenic Belt. *Earth Sci. Rev.* **208**, 103255 (2020).
40. Wang, X. X. et al. Nd-Hf isotopic mapping of Late Mesozoic granitoids in the East Qinling orogen, central China: Constraint on the basements of terranes and distribution of Mo mineralization. *J. Asian Earth Sci.* **103**, 169–183 (2015).
41. Wang, T. et al. Voluminous continental growth of the Altaids and its control on metallogeny. *Natl Sci. Rev.* **10**, nwac283 (2023).
42. Xu, Y. X. et al. Magnetotelluric imaging of a fossil oceanic plate in northwestern Xinjiang, China. *Geology* **48**, 385–389 (2020).
43. Bao, X. W., Song, X. D. & Li, J. T. High-resolution lithospheric structure beneath Mainland China from ambient noise and earthquake surface-wave tomography. *Earth Planet. Sci. Lett.* **417**, 132–141 (2015).
44. Zheng, Y. F., Zhao, Z. F. & Chen, R. X. Ultrahigh-pressure metamorphic rocks in the Dabie–Sulu orogenic belt: compositional inheritance and metamorphic modification. *Geol. Soc. Lond. Spec. Publ.* **474**, 89–132 (2018).
45. Condie, K. C. & Chomiak, B. Continental accretion: contrasting Mesozoic and Early Proterozoic tectonic regimes in North America. *Tectonophysics* **265**, 101–126 (1996).
46. Sylvester, P. J. Post-collisional strongly peraluminous granites. *Lithos* **45**, 29–44 (1999).
47. Mitchell, R. N., Kilian, T. M. & Evans, D. A. D. Supercontinent cycles and the calculation of absolute palaeolongitude in deep time. *Nature* **482**, 208–211 (2012).
48. Han, B. F. et al. Depleted mantle magma source for the Ulungur River A-type granites from North Xinjiang China: geochemistry and Nd–Sr isotopic evidence, and implication for Phanerozoic crustal growth. *Chem. Geol.* **138**, 135–159 (1997).
49. Kröner, A. et al. No excessive crustal growth in the Central Asian Orogenic Belt: further evidence from field relationships and isotopic data. *Gondwana Res.* **50**, 135–166 (2017).
50. Kusky, T. M. & Şengör, A. M. C. Comparative orotomy of the Archean Superior and Phanerozoic Altaid orogenic systems. *Natl Sci. Rev.* **10**, nwac235 (2023).
51. Niu, Y. L., Zhao, Z. D., Zhu, D. C. & Mo, X. X. Continental collision zones are primary sites for net continental crust growth — a testable hypothesis. *Earth Sci. Rev.* **127**, 96–110 (2013).
52. Collins, W. J., Murphy, J. B., Johnson, T. E. & Huang, H. Q. Critical role of water in the formation of continental crust. *Nat. Geosci.* **13**, 331–338 (2020).
53. Jacobsen, S. B. & Wasserburg, G. J. Sm-Nd isotopic evolution of chondrites and achondrites, II. *Earth Planet. Sci. Lett.* **67**, 137–150 (1984).
54. Arndt, N. T. & Goldstein, S. Use and abuse of crust-formation ages. *Geology* **15**, 893–895 (1987).

Acknowledgements

We are grateful for insightful reviews from Kent Condie, Long Chen and an anonymous reviewer. This work was supported by the National Key Technologies R&D Program (2019YFA0708600), the NSFC (grants 41830216 and 41888101), Science and Technology Major Project of Xinjiang Uygur Autonomous Region of China (2021A03001), and the Geological Survey Program of China (DD20190685). Thanks for the early reading of the MS and discussion by G.W. Zhang and C. van Staal and the data collection by S Li, L. Guo, C.Y. Cao, G.J. Zheng, and Z.X. Guo. This is a contribution to project IGCP 662 "Orogenic architecture and crustal growth from accretion to collision" and DDE (Deep-Time Digital Earth) Big Science Program.

Author contributions

T.W., W.X., and W.J.C. wrote the manuscript and in interaction with Y.T., C.W., X.W., H.H., Z.H., S.L., R. S., and B.H. collected and processed the main data. T.W. drew figures. W.X. shaped the tectonic implications of the study. C.W. and X.W. prepared Supplementary Data. All authors contributed to the writing and refinement of the final presentation.

Competing interests

The authors declare no competing interests.

Additional information

Supplementary information The online version contains supplementary material available at https://doi.org/10.1038/s43247-023-00779-5.

Correspondence and requests for materials should be addressed to Tao Wang or Wenjiao Xiao.

Peer review information *Communications Earth & Environment* thanks Kent Condie and the other, anonymous, reviewer(s) for their contribution to the peer review of this work. Primary handling editor: Joe Aslin. Peer reviewer reports are available.